Solar Energy Materials & Solar Cells 144 (2016) 411–417

Contents lists available at ScienceDirect

Solar Energy Materials & Solar Cells

journal homepage: www.elsevier.com/locate/solmat

Electrospraying-assisted rapid dye molecule uptake on the surfaces of TiO_2 nanoparticles for speeding up dye-sensitized solar cell fabrication

Xiuting Luo [a], Ji Hoon Kim [a], Ji Young Ahn [a], Dongyun Lee [a,c], Jong Man Kim [a,c], Dong Geun Lee [b,*], Soo Hyung Kim [a,c,**]

[a] Department of Nanofusion Technology, Pusan National University, 30 Jangjeon-dong, Geumjung-gu, Busan 609-735, Republic of Korea
[b] School of Mechanical Engineering, Pusan National University, 30 Jangjeon-dong, Geumjung-gu, Busan 609-735, Republic of Korea
[c] Department of Nano Energy Engineering, Pusan National University, 30 Jangjeon-dong, Geumjung-gu, Busan 609-735, Republic of Korea

ARTICLE INFO

Article history:
Received 18 April 2015
Received in revised form
24 September 2015
Accepted 25 September 2015

Keywords:
Electrospraying process
Dye adsorption
Photocatalytic nanoparticles
Electrostatic attraction forces
Dye-sensitized solar cells

ABSTRACT

In this paper, we propose a versatile electrospraying method that allows for the rapid uptake of dye molecules on the surfaces of TiO_2 nanoparticles (NPs) for speeding up the fabrication of dye-sensitized solar cells (DSSCs). The proposed method both significantly speeds up the dye molecule adsorption process and increases the amount of dye adsorbed. We systematically investigated the effects of the applied voltage and the substrate heating temperature during the electrospraying of the dye-molecule-containing solution on the photovoltaic performance of the resulting DSSCs in terms of their open-circuit voltage, short-circuit current, fill factor, and power conversion efficiency (*PCE*). The electrospraying method reduced the length of the dye adsorption process by several hours and is almost 10 times faster than the conventional dip-coating method for depositing dye molecules on the surfaces of the TiO_2 NPs in the photoelectrodes of DSSCs. This was because of the electrostatic force of attraction between the dye molecules and the TiO_2 NPs. The *PCE* of the resulting DSSCs (4.68% for a photoactive area of 0.36 cm^2), which were assembled by electrospraying for 3 h, was higher than that of DSSCs assembled by dip coating for 30 h (4.28% for a photoactive area of 0.36 cm^2), owing to the fact that the amount of dye adsorbed in the former case was much higher.

1. Introduction

Dye-sensitized solar cells (DSSCs), which were first proposed by Grätzel et al. [1], are composed of a TiO_2-thin-film-coated fluorine-doped tin oxide (FTO) photoelectrode, a dye, an electrolyte (I^-/I_3^- redox couple), and a Pt-thin-film-coated counter electrode. These cells have come to be regarded as next-generation solar cells because of their relatively high power conversion efficiency (*PCE*), simple fabrication process, low cost, and short energy payback [1–5].

The working principle of DSSCs is as follows. Dye molecules are attached to the surfaces of the TiO_2 semiconducting nanoparticles (NPs) in the photoelectrode. When the DSSC is exposed to sunlight, electrons generated from the excited dye molecules are injected into the conduction band of the TiO_2 NPs and reach the conducting oxide electrode (e.g., fluorine-doped tin oxide (FTO)). Next, the photogenerated electrons flow through the external circuit and are reintroduced into the Pt-coated counter electrode, flowing into the liquid electrolyte. The electrolyte finally transports the electrons, completing a current cycle.

Significant efforts have been devoted to improving the photovoltaic performance of DSSCs by optimizing their various parts, including the photoelectrode [6–11], photosensitizer [12–14], redox electrolyte [15,16], and counter electrode [17,18]. Among the various components of DSSCs, the photoelectrode takes the longest to fabricate. It is made by printing a porous TiO_2 thin film on the surface of a FTO glass substrate, which is then immersed into a bath of the dye solution for 10–36 h to ensure adequate dye adsorption [19,20]. This dip-coating-based dye adsorption process does not allow for the rapid fabrication of DSSCs. In addition, having to repeat the dip-coating process in order to produce DSSCs on a large scale can result in the continuous consumption of a large amount of the dye. This can cause a significant decrease in the concentration of the dye molecules in the solution. Thus, the sustainability and stability of the photovoltaic performance of the resulting DSSCs can be difficult to maintain.

In order to reduce the time taken for the dye-adsorption process during DSSC fabrication, several research groups have suggested

* Corresponding author.
** Corresponding author at: Department of Nanofusion Technology, Pusan National University, 30 Jangjeon-dong, Geumjung-gu, Busan 609-735, Republic of Korea.
E-mail addresses: donglee@pusan.ac.kr (D.G. Lee), sookim@pusan.ac.kr (S.H. Kim).

http://dx.doi.org/10.1016/j.solmat.2015.09.042
0927-0248/

approaches to increase the dye-adsorption rate. These approaches increase the dye diffusion flux considerably by using dye solutions with high concentrations at high temperatures [21] and by employing high reflux pumping [22] and high-speed solution droplet bombardment [23]. However, all of these approaches have inherent difficulties in realizing large-area DSSCs with controlled degrees of dye adsorption. In this study, we demonstrate a rapid dye-adsorption process based on electrospraying that shortens the dye-adsorption time by several hours and simultaneously increases the amount of dye adsorbed through an electrostatic refluxing process, such that the photovoltaic performance of the resulting DSSCs is much better than that of those assembled using the conventional dip-coating process.

2. Experimental details

2.1. Preparation of photoelectrode

Commercial TiO_2 NPs (P25, Degussa, Germany) were used without further treatment. To prepare a TiO_2 paste, a solution (called solution 1) consisting of 6 g of the TiO_2 NPs, 1 ml of acetic acid (CH_3COOH), 20 g of terpineol, and 15 g of ethanol was formed in vial. Next, another solution (called solution 2) consisting of 3 g of ethyl cellulose and 27 g of ethanol was formed in another vial. Then, solutions 1 and 2 were sonicated for 1 h each and homogeneously mixed in a single vial using a planetary mixer for 3 min. The mixture was then heated to evaporate the ethanol. Using screen printing, a thin film of TiO_2 was formed on a FTO glass substrate (SnO_2/F, 7 Ω/sq, Pilkington, Boston, USA) with a photoactive area of 0.6 cm × 0.6 cm and thickness of 20 μm. The FTO glass substrate was cleaned using acetone, ethanol, and deionized water and then pretreated with a mixture consisting of 0.247 ml of a $TiOCl_2$ solution and 20 ml of deionized water to improve the adhesion of the TiO_2 NPs on it. It was then thermally treated at 500 °C for 30 min. The TiO_2-thin-film-coated FTO glass substrate was then sintered again at 500 °C for 30 min in order to remove the residual components. Another FTO glass substrate was used as the counter electrode; two holes were drilled into it and the substrate was cleaned. It was then coated with Pt by ion sputtering (Model no. E1010, Hitachi, Chiyoda-ku, Japan).

2.2. Dye adsorption on the TiO_2 thin film and fabrication of DSSCs

An electrospraying device was employed to deposit the dye solution. Different high voltages were applied to the syringe tip. The syringe was filled with the dye-molecule-containing solution. The surface of the dye solution was subjected to an electrical

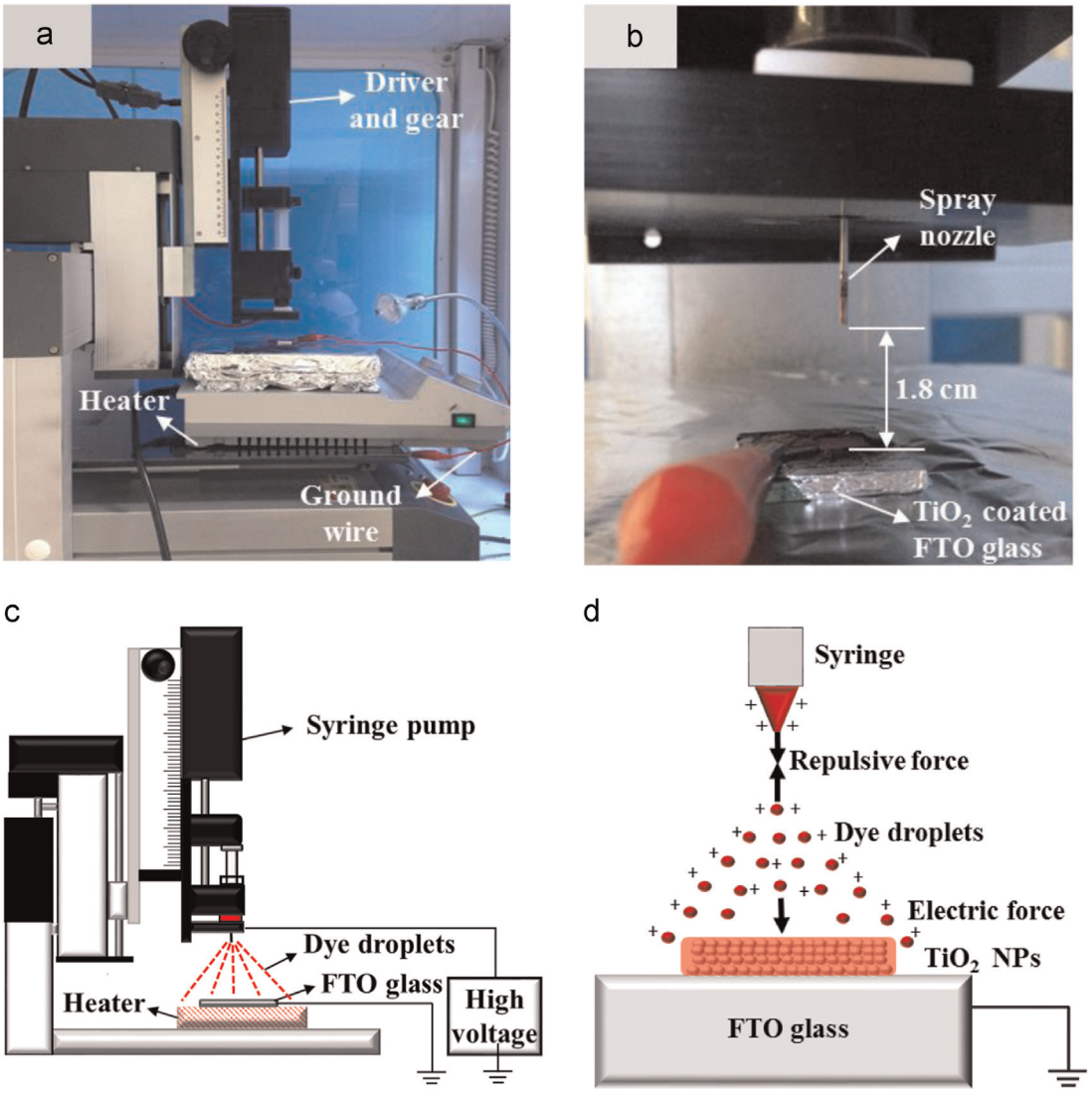

Fig. 1. (a) Side-view and (b) close-up photographs and (c) schematic diagram of the electrospraying device and (d) schematic of the mechanism for depositing the dye-containing liquid droplets on the surfaces of the TiO_2 NPs using the electrospraying system.

stress, and it deformed to form an elongated jet, which was disrupted into positively charged dye-contained droplets [24]. The FTO glass substrate coated with the TiO_2 thin film was installed below the syringe tip; the substrate was electrically grounded, as shown in Fig. 1. Under the applied electric force, the dye-containing droplets were attracted to the porous TiO_2 thin film and continuously permeated through the interstitial space between the porous TiO_2 NPs; the carboxylate (–COOH) groups of the dye molecules bonded with the hydroxyl (–OH) groups on the surfaces of the TiO_2 NPs, resulting in ester linkages.

The electrospray-assisted adsorption of the dye on the TiO_2-NP-coated FTO glass substrate is shown in Fig. 1; the FTO glass substrate was covered with an aluminum foil mask and the syringe was filled with a dye solution containing 0.3 mM of Ru-dye $(Bu_4N)_2[Ru(Hdcbpy)_2–(NCS)_2]$ (N719, Solaronix, SA, Switzerland). The distance between the syringe tip and the FTO glass substrate was fixed at 1.8 cm, and the dye solution flow rate was fixed at 80 μL min^{-1}. As mentioned above, the dye solution was disrupted into positively charged droplets and sprayed on the TiO_2 thin film. In addition, a heater was installed under the FTO glass substrate to adjust the temperature in order to evaporate the deposited dye-containing droplets. After the completion of the dye-adsorption process, any remaining dye was washed away with ethanol, and the substrate was dried in a convection oven at 80 °C. Both the photoelectrode and the counter electrode were then sealed with a hot-melt polymer film (60 μm in thickness, Surlyn, DuPont, USA) in a sandwich-type configuration and heated at 120 °C for 4 min. Next, an iodide-based liquid electrolyte (AN-50, Solaronix, SA, Switzerland) was injected between the two electrodes, yielding an assembled DSSC.

2.3. Characterization of photovoltaic performance of DSSCs

The photovoltaic performance of the thus-fabricated DSSCs was measured under air mass 1.5 and 1 sun (=100 mW/cm^2) illumination using a solar simulator (PEC-L11, Peccell Technologies, Inc., Kanagawa, Japan). The current density–voltage (*J–V*) curves and electrochemical impedance spectroscopy (EIS) curves were recorded automatically with a Keithley SMU 2400 source meter (Cleveland, OH, USA). The amount of dye adsorbed onto the TiO_2 thin film was determined using an Ultraviolet–visible (UV–vis) spectrometer (Cary 5000, Agilent, Englewood, CA, USA); the substrate was first washed with a 0.1 mol/L NaOH solution (deionized water:ethanol=1:1) and the absorbance of the dye solution was measured [25].

3. Results and discussion

Fig. 2 shows the various electrospraying modes corresponding to the different applied voltages, which ranged from 5 kV to 14 kV; the dye solution flow rate was fixed at 80 μL/min. For applied voltages of 5 kV and 6 kV, no droplets were generated, and only a liquid jet flowed vertically; this was true even in the con-jet mode. When the applied voltage reached 7 kV, microdripping [26] and liquid droplets were generated. When the applied voltage was increased beyond 7 kV, multiple jets were formed, and the size of liquid droplets decreased significantly.

It is also important to control the temperature of the FTO glass substrate, as it is necessary to ensure that the dye-molecule-containing droplets do not evaporate and can readily permeate through the TiO_2 NPs in the photoelectrode of the DSSCs [27]. We systematically investigated the effects of the applied voltage and the substrate temperature on the photovoltaic performance of the resulting DSSCs, as shown in Fig. 3. All the DSSCs involved electrospraying the dye-molecule-containing droplets for 30 min. As shown in Fig. 3, the *PCE* of the DSSCs increased significantly for applied voltages of 7–9 kV and then decreased suddenly at 10 kV at temperatures of 20–40 °C. This suggests that the dye-containing droplets effectively penetrated through and were adsorbed onto the TiO_2 NPs while in the liquid state. However, the initial size of the droplets was too small at voltages higher than 10 kV. As a result, they dried because of rapid evaporation, and the dye in them turned solid before being deposited on the surfaces of the TiO_2 NPs. When the substrate temperature was increased to 50–70 °C, the *PCE* of the DSSCs decreased linearly with an increase in the applied voltages. This suggests that the liquid droplets evaporated rapidly and the dye in them turned solid at higher temperatures. This made the dye remain on the surfaces of the TiO_2 thin film and not permeate through the TiO_2 NPs. We employed a fixed applied voltage of ~9 kV and a temperature of 20 °C as the optimized electrospraying conditions for all later experiments.

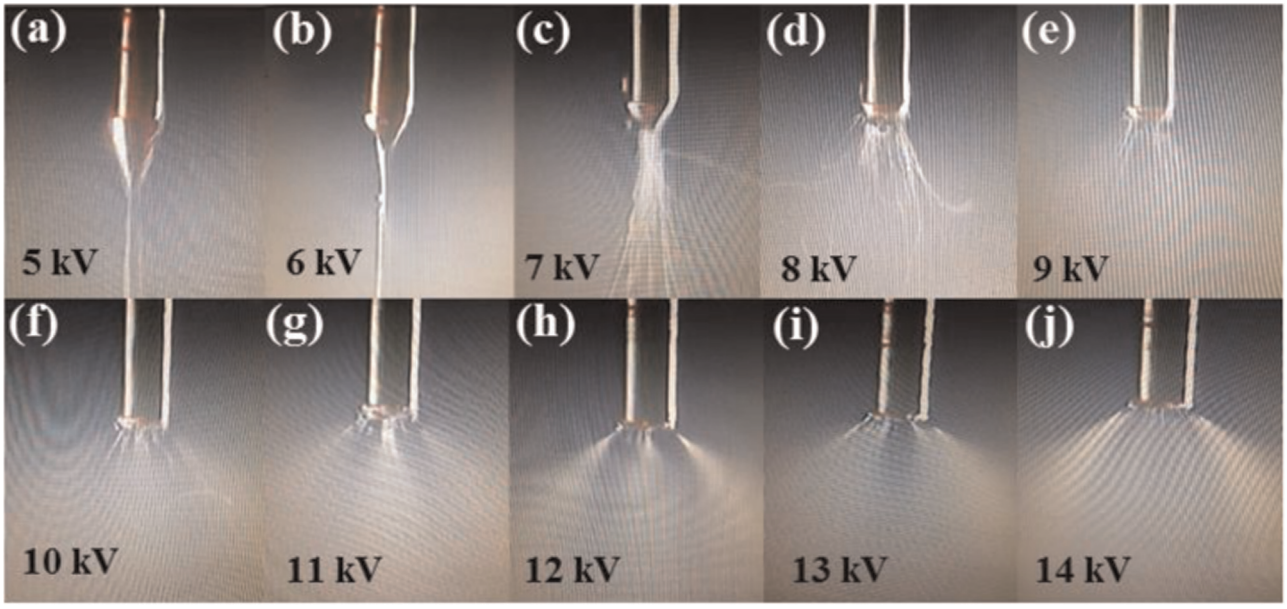

Fig. 2. Photographs of the various electrospraying modes corresponding to applied voltages of (a) 5 kV, (b) 6 kV, (c) 7 kV, (d) 8 kV, (e) 9 kV, (f) 10 kV, (g) 11 kV, (h) 12 kV, (i) 13 kV, and (j) 14 kV. The flow rate of the dye-containing solution was fixed at ~80 μL/min.

Using an applied voltage of ~9 kV and temperature of 20 °C, we investigated the effects of the electrospraying time on the photovoltaic performance of the fabricated DSSCs. For comparison, we also fabricated DSSCs using the conventional dip-coating method for various dip-coating times. As can be seen from Table 1, the amount of dye adsorbed (M_{DA}), short-circuit current density (J_{sc}), and *PCE* increased linearly with an increase in both the dip-coating time and the electrospraying time, eventually plateauing at a saturation point. The M_{DA} and J_{sc} values for the DSSC assembled by electrospraying for 3 h were 15.83×10^{-6} mol/cm^2 and 10.00 mA/cm^2; in contrast, those for the DSSC fabricated by dip coating for 30 h were 9.44×10^{-6} mol/cm^2 and 8.94 mA/cm^2. The highest *PCE* for the DSSCs fabricated by electrospraying was 4.68%; this was much higher than that for the dip-coating-fabricated DSSCs (4.28%). This suggests that one can reduce the dye adsorption time by as much as a factor of ten and increase the amount of dye adsorbed by using the electrospraying method. The stability of DSSCs assembled by electrospraying process can also be improved because the dye molecules were strongly attached to the surface of TiO_2 NPs by electrostatic attraction forces.

The open-circuit voltage (V_{oc}) also increased gradually with an increase in the dip-coating time and the electrospraying time, because it depends mainly on the number of electrons injected into the TiO_2 conduction band [28]. The fill factor (*FF*) can be defined as follows:

$$FF = \frac{V_{max} \cdot J_{max}}{V_{oc} \cdot J_{sc}} \quad (1)$$

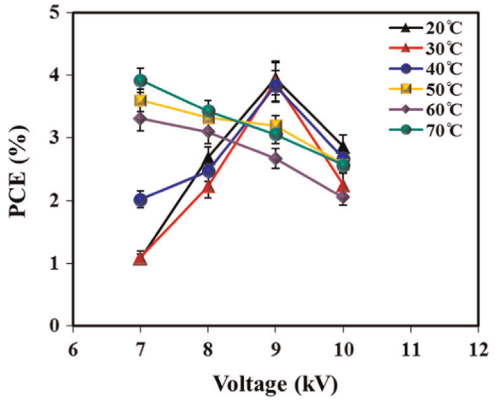

Fig. 3. Evolution of the *PCE* value of the DSSCs assembled using the electrospraying-assisted dye-deposition method as functions of the applied voltage and the substrate temperature for a fixed electrospraying time of 30 min.

where V_{max} and J_{max} are the voltage and current density corresponding to the maximum power. The *FF* decreased slightly with an increase in V_{oc} and J_{sc}.

Fig. 4a and b shows the *J*–*V* curves of the DSSCs assembled using different dip-coating times and electrospraying times, respectively. With an increase in both the dip-coating time and the electrospraying time, the maximum power increased significantly, owing to the fact that larger amounts of the dye were adsorbed. From the Nyquist plots shown in Fig. 4c and d, one could calculate the recombination resistance (R_{rec}) and the transport resistance (R_t). Here, R_{rec} is the resistance between the TiO_2/dye/electrolyte interfaces and is determined by the length of the second semicircle in the shown Nyquist plots. It can be seen that the R_{rec} value for the DSSCs fabricated by electrospraying was much smaller than that for the DSSCs fabricated by dip coating. This is because the TiO_2 thin film could adsorb a greater number of dye molecules when they were deposited by the electrospraying method. This resulted in an increase in the number of photogenerated electrons, which increased J_{sc} and lowered R_{rec}, as shown in Fig. 4c and d and Table 1. Further, R_t is the electron-transport resistance between the TiO_2 NPs and the resistance between the TiO_2 thin film and the FTO glass substrate [29]; it can be calculated as follows:

$$R_t/3 + R_{rec} = R_{total} \quad (2)$$

where R_{total} is the total resistance of the cell.

As can be seen from Table 1, R_t was observed to increase slightly with the increase in the dye adsorption time; this was true for both dip coating and electrospraying. It also resulted in a decrease in the *FF* value. It is obvious that longer dye adsorption times result in the formation of dense aggregates of the dye molecules within the TiO_2 thin films, which would hinder the photogenerated electrons from being transported through the TiO_2 layer and reaching the FTO glass substrate. In other words, a thicker layer of the dye molecules would perturb the transport of the photogenerated electrons from the TiO_2 layer to the FTO glass substrate.

From the Bode plots shown in Fig. 4e and f, one can calculate the electron lifetime (τ_e) as follows:

$$\tau_e = \frac{1}{2\pi f_{max}} \quad (3)$$

where f_{max} is the maximum peak frequency.

The electron lifetime increased with an increase in the electrospraying time, suggesting that a greater number of the photogenerated electrons diffused further, owing to the amount of dye adsorbed being higher.

Table 1
Photovoltaic performances of N719 dye deposited using the conventional dip-coating method for different dip-coating times and the electrospraying method for a fixed voltage of 9 kV and substrate temperature of 20 °C for different electrospraying times.

Dye adsorption method	Time (min)	M_{DA} (10^{-6} mol/cm^2)	J_{sc} (mA/cm^2)	V_{oc} (V)	*FF*	*PCE* (%)	R_{rec} (Ω)	R_t (Ω)	τ_e(ms)
Dip coating	60	1.56	3.73	0.60	0.74	1.64	24.64	3.69	0.50
	300	5.28	4.83	0.63	0.72	2.22	13.82	3.94	0.63
	600	5.56	7.70	0.62	0.72	3.32	10.40	4.01	1.26
	1200	8.61	8.12	0.63	0.72	4.00	9.57	4.05	1.26
	1800	9.44	8.94	0.68	0.70	4.28	8.89	4.53	2.52
Electrospraying	10	5.36	4.92	0.61	0.74	2.23	13.89	4.92	0.80
	20	5.44	5.13	0.61	0.74	2.31	13.15	5.15	1.00
	30	7.78	7.48	0.63	0.73	3.42	9.62	5.72	1.30
	60	9.14	8.41	0.65	0.72	3.91	9.36	5.85	1.70
	120	12.56	9.76	0.64	0.72	4.32	8.77	6.32	3.10
	150	14.64	9.85	0.65	0.71	4.65	8.61	6.54	4.00
	180	15.83	10.00	0.66	0.71	4.68	7.92	7.03	4.00

*Note: M_{DA}: amount of dye adsorbed, J_{sc}: short-circuit current, V_{oc}: open-circuit voltage, *FF*: fill factor, *PCE*: power-conversion efficiency, R_{rec}: recombination resistance, R_t: transport resistance, τ_e: electron lifetime.

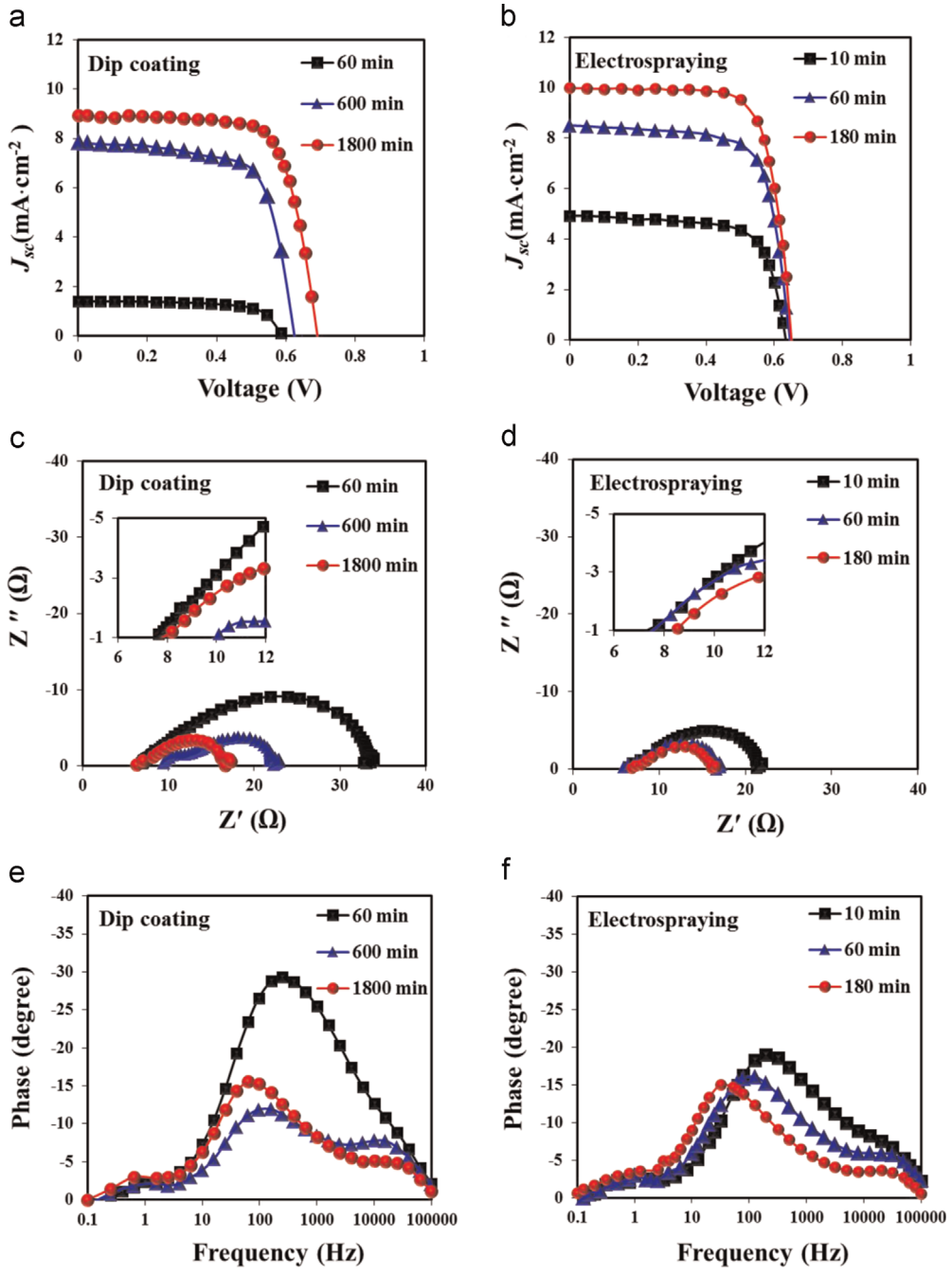

Fig. 4. (a) *J–V* curves, (c) Nyquist plots, (e) Bode plots of the DSSCs assembled by the dip-coating method for different dip-coating times and (b) *J–V* curves, (d) Nyquist plots, (f) Bode plots of the DSSCs assembled using the electrospraying method for different electrospraying times.

To determine the primary factor responsible for the observed improvement in the *PCE* of the DSSCs fabricated by electrospraying, the incident photon-to-electron conversion efficiency (*IPCE*) spectra of the DSSCs were measured as functions of the incident-light wavelength. As shown in Fig. 5, the *IPCE* spectra indicated that the electrospraying-fabricated DSSC exhibited a higher *IPCE* for an electrospraying time of more than 60 min than did the DSSC fabricated by dip coating for 1800 min. This further confirmed that electrospraying is an effective and rapid dye-deposition method and can enhance the photovoltaic performance of DSSCs.

Fig. 6a shows photographs of the DSSCs assembled by conventional dip coating and electrospraying for different processing times. It can be seen clearly that the color of the DSSCs became deeper with an increase in the dip-coating and electrospraying times, with the deepest color being observed for an electrospraying time of 180 min. Further, Fig. 6b shows that the electrospraying method can significantly reduce the duration of the dye adsorption process by a factor of 10 and that one can achieve *PCE* values higher than those of dip-coated DSSCs, as a greater amount of dye is adsorbed in the case of electrospraying because of the electrostatic force of attraction between the dye molecules and the TiO_2 NPs in the photoelectrode.

4. Conclusions

In this study, we demonstrated rapid dye deposition for DSSC fabrication using an electrospraying method that enabled us to

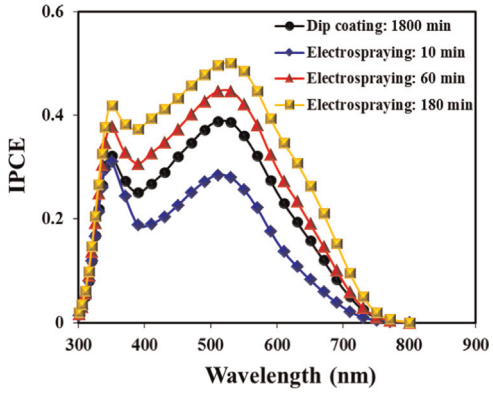

Fig. 5. Incident photon-to-electron conversion efficiency (*IPCE*) spectra of the DSSCs fabricated using the electrospraying method for different electrospraying times and the DSSC assembled by the dip-coating method for 30 h; the latter device exhibited the best photovoltaic performance of all the DSSCs assembled using the dip-coating method.

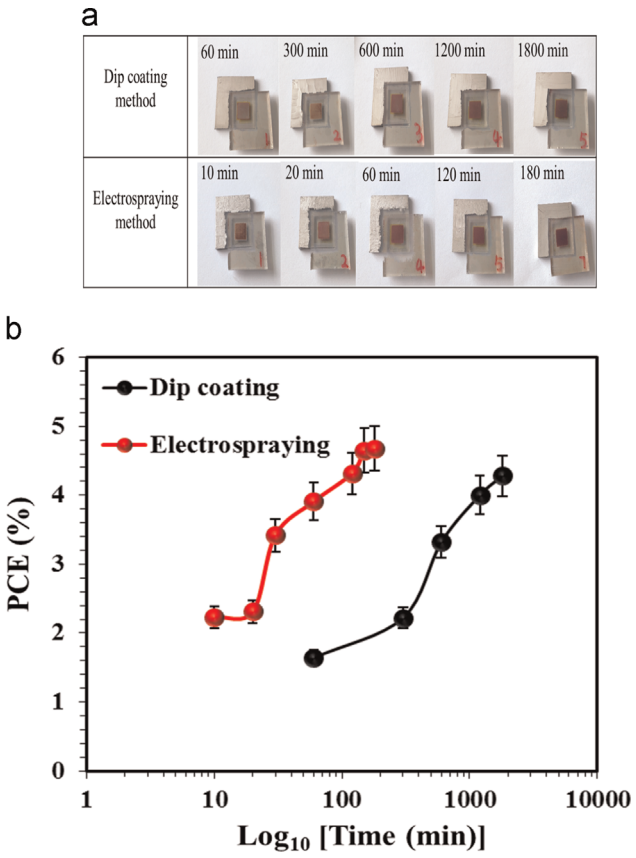

Fig. 6. (a) Photographs of the DSSCs assembled using different dip-coating and electrospraying times and (b) comparison of the *PCE* values of the DSSCs assembled using different electrospraying and dip-coating times.

significantly reduce the dye adsorption time and simultaneously increase the amount of dye adsorbed. Specifically, we first systematically examined the different electrospraying modes resulting from the use of different voltages and substrate heating temperatures and optimized the electrospraying conditions for the adsorption of the dye molecules on the TiO_2 NPs. These were determined to an applied voltage of ~9 kV and a temperature of 20 °C; under these conditions, the dye-containing droplets could reach the surfaces of the TiO_2 thin film in the liquid state and permeate through the TiO_2 thin film to a degree sufficient to allow them to be absorbed on the surfaces of the TiO_2 NPs. Further, we found that the electrospraying method also significantly increased the photovoltaic performance of DSSCs by increasing the amount of dye adsorbed, which was because of the electrostatic force of attraction between the dye molecules and TiO_2 NPs. The electrospraying method proposed in this study can potentially accelerate the industrial processes for manufacturing DSSCs as well as improve their photovoltaic performance. This is because it leads to strong adhesion between the dye molecules and the semiconducting oxide NPs and simultaneously increases the amount of dye adsorbed and decreases the deposition time.

Acknowledgment

This study was supported by the Global Frontier R&D Program of the Center for Multiscale Energy System, funded by the National Research Foundation, which is supported by the Ministry of Education, Science and Technology, Korea (2012M3A6A7054863).

References

[1] B. O'Regan, M. Grätzel, A low-cost, high-efficiency solar cell based on dye sensitized colloidal TiO_2 films, Nature 353 (1991) 737.
[2] B. O'Regan, M. Grätzel, D. Fitzmaurice, Optical electrochemistry **I**: steady-state spectroscopy of conduction-band electrons in a metal oxide semiconductor electrode, Chem. Phys. Lett. 183 (1991) 89–93.
[3] M. Grätzel, Photoelectrochemicla cells, Nature 414 (2001) 338–344.
[4] A. Hagfeldt, M. Grätzel, Molecular photovoltaics, Acc. Chem. Res. 33 (2000) 269–277.
[5] P. Wang, S.M. Zakeeruddin, J.E. Moser, M.K. Nazeeruddin, T. Sekifuchi, M. Grätzel, A stable quasi-solid-state dye-sensitized solar cell with an amphiphilic ruthenium sensitizer and polymer gel electrolyte, Nat. Mater. 402 (2003) 402–407.
[6] Y. Gao, M. Nagai, Morphology evolution of ZnO thin films from aqueous solutions and their application to solar cells, Langmuir 22 (2006) 3936.
[7] K.J. Moon, S.W. Lee, Y.H. Lee, J.H. Kim, J.Y. Ahn, S.J. Lee, D.W. Lee, S.H. Kim, Effect of TiO_2 nanoparticle-accumulated bilayer photoelectrode and condenser lens-assisted solar concentrator on light harvesting in dye- sensitized solar cells, Nanoscale Res. Lett. 8 (2013) 283.
[8] J.Y. Ahn, J.H. Kim, K.J. Moon, S.D. Park, S.H. Kim, Synergistic effects of the aspect ratio of TiO_2 nanowires and multi-walled carbon nanotube embedment for enhancing photovoltaic performance of dye-sensitized solar cells, Nanoscale 5 (2013) 6842.
[9] Q. Li, J. Wu, Q.W. Tang, Z. Lan, P.J. Li, J.M. Lin, L.Q. Fan, Application of microporous polyaniline counter electrode for dye-sensitized solar cells, Electrochem. Commun., 10, (2008) 1299–1302.
[10] A. Latini, C. Cavallo, F.K. Aldibaja, D. Gozzi, Efficiency improvement of DSSC photoanode by scandium doping of mesoporous titania beads, J. Phys. Chem. C 117 (2013) 25276–25289.
[11] J.Y. Ahn, K.J. Moon, J.H. Kim, S.H. Lee, J.W. Kang, H.W. Lee, S.H. Kim, Designed synthesis and stacking architecture of solid and mesoporous TiO_2 nanoparticles for enhancing the light-harvesting efficiency of dye-sensitized solar cells, ACS Appl. Mater. Int. 6 (2014) 903–909.
[12] L.H. Han, C.R. Zhang, J.W. Zhe, N.Z. Jin, Y.L. Shen, W. Wang, J.J. Gong, Y.H. Chen, Z.J. Liu, Understanding the electronic structures and absorption properties of porphyrin sensitizers YD2 and YD2-o-C8 for dye-sensitized solar cells, Int. J. Mol. Sci 14 (2013) 20171–20188.
[13] E.M. Barea, J. Ortiz, F.J. Payá, F.F. Lázaro, F.F. Sangtiago, A.S. Santos, J. Biquert, Energetic factors governing injection, regeneration and recombination in dye solar cells with phthalocyanine sensitizers, Energy Environ. Sci. 3 (2010) 1985–1994.
[14] A. Krkrek, D. Wang, Y. Hou, R. Zong, R. Thummel, Photosensitizers containing the 1,8-Naphthyridyl moiety and their use in dye-sensitized solar cells, ACS. Inorg. Chem., 45, (2006) 10131–10137.
[15] P. Suri, R.M. Mehra, Effect of electrolyte on the photovoltaic performance of a hybrid dye sensitized ZnO solar cell, Sol. Energy Mater. Sol. Cells 91 (2007) 518–524.
[16] J. Wu, Z. Lan, S. Hao, P.J. Li, J.M. Lin, M.L. Huang, L. Fang, Y. Huang, Progress on the electrolytes for dye-sensitized solar cells, Pure Appl. Chem. 80 (2008) 2241–2258.
[17] J.Y. Ahn, J.H. Kim, J.M. Kim, D. Lee, S.H. Kim, Multiwalled carbon nanotube thin films prepared by aerosol deposition process for use as highly efficient Pt-free counter electrodes of dye-sensitized solar cells, Sol. Energy 107 (2014) 660–667.
[18] H. Wang, Y.H. Hu, Graphene as a counter electrode material for dye-sensitized solar cells, Energy Environ. Sci. 5 (2012) 8182.

[19] K.E. Jasim, L.A. Kosyanchenko (Eds.), Dye Sensitized Solar Cells–Working Principles, Challenges and Opportunities, Solar Cells–Dye–Sensitized Devices, In Tech Europe, Rijeka, Croatia, 2011, ISBN: 978-953-307-735-2.
[20] T. Tesfamichael, G. Will, J. Bell, K. Prince, N. Dytlewski, Characterization of a commercial dye-sensitized titania solar cell electrode, Sol. Energy Mater. Sol. Cells 76 (2003) 25–35.
[21] J.M. Chern, C.Y. Wu, Desorption of dye from activated carbon beds: Effects of temperature pH, and alcohol, Water Res. 35 (2001) 4159–4165.
[22] A. Hinsch, J.M. Kroon, R. Kern, I. Uhlendorf, J. Holzbock, A. Meyer, J. Ferber, Long-term stability of dye-sensitized solar cells, Prog. Phorovolt: Res. Appl. 9 (2001) 425–438.
[23] H.P. Kuo, C.T. Wu, Speed up dye-sensitized solar cell fabrication by rapid dye solution droplets bombardment, Sol. Energy Mater. Sol. Cells 120 (2014) 81–86.
[24] M. Cloupeau, B.P. Foch, Electroohydrodynamic spraying function modes: A critical review, J. Aerosol Sci. 6 (1994) 1021–1036.
[25] H. Yu, S.Q. Zhang, H. Zhao, H. Zhang, Photoelectrochemical quantification of electron transport resistance of TiO_2 photoanodes for dye-sensitized solar cells, Phys. Chem. Chem. Phys. 12 (2010) 6625–6631.
[26] A. Jaworek, Micro- and nanoparticle production by electrospraying, Powder Technol. 176 (2007) 18–35.
[27] B. Kim, S.W. Park, J.Y. Kim, K. Yoo, J.A. Lee, M.W. Lee, D.K. Lee, J.Y. Kim, B.S. Kim, H. Kim, S. Han, H.J. Son, M.J. Ko, Rapid dye adsorption via surface modification of TiO_2 photoanodes for dye-sensitized solar cells, ACS Appl. Mater. Int., 5, (2013) 5201–5207.
[28] F.D. Angelis, S. Fantacci, A. Selloni, M. Grätzel, M.K. Nazeeruddin, Influence of the sensitized adsorption mode on the open-circuit potential of dye-sensitized solar cells, Nano Lett. 7 (2007) 3189–3195.
[29] J. Bisquert, F.F. Santiago, I.M. Seró, G.G. Belmonte, S. Giménez, Electron lifetime in dye-sensitized solar cells: theory and interpretation of measurements, J. Phys. Chem. C 113 (2009) 17278–17290.